Passive detection of vehicle loading

Troy R. McKay[a], Carl Salvaggio[a], Jason W. Faulring[a], Philip S. Salvaggio[a], Donald M. McKeown[a], Alfred J. Garrett[b], David H. Coleman[b], Larry D. Koffman[b]

[a]Rochester Institute of Technology, College of Science, Chester F. Carlson Center for Imaging Science, 54 Lomb Memorial Drive, Rochester, NY, USA
[b]Savannah River National Laboratory, Building 735-A, Office B108, Aiken, SC, USA

ABSTRACT

The Digital Imaging and Remote Sensing Laboratory (DIRS) at the Rochester Institute of Technology, along with the Savannah River National Laboratory is investigating passive methods to quantify vehicle loading. The research described in this paper investigates multiple vehicle indicators including brake temperature, tire temperature, engine temperature, acceleration and deceleration rates, engine acoustics, suspension response, tire deformation and vibrational response. Our investigation into these variables includes building and implementing a sensing system for data collection as well as multiple full-scale vehicle tests. The sensing system includes; infrared video cameras, triaxial accelerometers, microphones, video cameras and thermocouples. The full scale testing includes both a medium size dump truck and a tractor-trailer truck on closed courses with loads spanning the full range of the vehicle's capacity. Statistical analysis of the collected data is used to determine the effectiveness of each of the indicators for characterizing the weight of a vehicle. The final sensing system will monitor multiple load indicators and combine the results to achieve a more accurate measurement than any of the indicators could provide alone.

Keywords: heavy vehicle, brake temperature, tire temperature, engine temperature, acceleration, deceleration, engine acoustics, vehicle stability, suspension response, tire deformation, vibrational response

1. INTRODUCTION

A fully loaded vehicle will behave differently than an unloaded or partially loaded vehicle. This is true of the overall vehicle system as well as many related vehicle subsystems. These operational deviations by both the vehicle system and the vehicle subsystems produce multiple indicators of loading. This section will briefly describe the vehicle system and subsystems and how they are affected by vehicle weight.

The amount of thermal energy generated by the braking system is affected by the amount of load the vehicle is carrying. A vehicle being operated with a high load will have more kinetic energy than the same vehicle carrying a standard load traveling at the same velocity. If a standard friction style braking system is employed, more thermal energy would be generated by the vehicle being operated with a high load than would be generated by a vehicle carrying a lesser load. Assuming the vehicle's kinetic energy is converted directly to heat by the braking system, the thermal energy generated can be described by the relationship[1]

$$E_b = \frac{m}{2}\left(V_1^2 - V_2^2\right) + \frac{I}{2}\left(\omega_1^2 - \omega_2^2\right) \tag{1}$$

where E_b denotes the thermal energy generated by the brakes, V_1 the velocity of the vehicle prior to braking, V_2 the velocity of the vehicle after braking, I the moment of inertia of the vehicle's drivetrain, ω_1 the angular velocity of the drivetrain prior to braking and ω_2 the angular velocity of the drivetrain after braking.

The amount of thermal energy generated by the vehicle's tires interacting with the road surface is affected by the amount of weight the vehicle is carrying. When a standard rubber tire interacts with the road surface while driving, the rubber deforms. The deformation of the rubber tire beyond its elastic limits generates thermal

Further author information: Send correspondence to Troy McKay: trm8945@cis.rit.edu, 585.739.3163 (voice)

Visual Information Processing and Communication III, edited by Amir Said, Onur G. Guleryuz, Robert L. Stevenson,
Proc. of SPIE-IS&T Electronic Imaging Vol. 8305, 830511 · © 2012 SPIE-IS&T
CCC code: 0277-786X/12/$18 · doi: 10.1117/12.912100

energy. As the vehicle load increases, the amount of tire deformation also increases in turn causing more thermal energy to be generated.

The amount of thermal energy generated by the vehicle's rear differential is affected by the amount of load the vehicle is carrying. The purpose of a vehicle's rear differential is to transmit energy from the engine to the drive train wheels. A standard rear differential consists of a set of gears that takes an input torque and rotation via the driveshaft and provides torque and rotation to the drive wheels. Thermal energy is generated within the rear differential through friction between the gears. The amount of friction generated by the rear differential increases with the amount of load the vehicle is carrying. This thermal energy can help to characterize the amount of load a vehicle is carrying.

The amount of thermal energy generated by the vehicle's engine is affected by the amount of load the vehicle is carrying. The engine will need to operate at a higher speed (RPM) to achieve the same acceleration rates when the vehicle is carrying a full load compared to when the vehicle is carrying a partial load. As an engine is operated at a higher frequency the engine's combustion rate increases, which in turn causes the amount of heat generated by the engine to increase. Additionally, the acoustic signal generated by the engine provides an indicator directly related to the frequency at which the engine is being operated.

The acceleration rate of a vehicle is affected by the amount of weight the vehicle is carrying. The acceleration rate of a fully loaded vehicle will be less than that of a vehicle carrying a partial load for the same transmission gear and engine rotations per minute (RPM). Similarly, the deceleration rate of a fully loaded vehicle will be less than that of a vehicle carrying a partial load given the same braking system and application method.

The suspension system of a vehicle is affected by the amount of weight the vehicle is carrying. The suspension system for most vehicles acts as a damped spring coupler between the frame of the vehicle, where the load would be located, and the vehicle's axles. As a vehicle travels over bumps, oscillations are induced in the suspension system, the amplitude and level of damping of which vary for the same vehicle carrying different loads.

The amount of tire deformation of a vehicle is affected by the amount of weight the vehicle is carrying. A standard tire is composed of an elastic material, usually rubber, pressurized with a gas, usually air. The tires completely support the weight of the vehicle and its load. The amount of tire deformation will be larger for a fully loaded vehicle than for a vehicle carrying a partial load.

The vibration induced by a vehicle onto the medium over which it is travelling is affected by the amount of weight the vehicle is carrying. When a vehicle is traveling over a road surface, vibrations are induced by its travel. Particularly, when a vehicle is traversing an object such as a speed bump or a railroad track, more vibrational energy will be transmitted to the object for a vehicle carrying a full load than that of the same vehicle carrying a partial load.

Each of these indicators alone could give an observer information about the weight of the vehicle, however, due to the large number of unknown variables associated with any given vehicle, this information on its own would most likely not be enough to accurately determine the vehicle weight. Combining the measurements of the indicators with the strongest correlation to vehicle weight should produce more accurate weight estimates.

2. EXPERIMENTAL APPROACH

In order to better quantify the relationship between the weight of a loaded vehicle and the indicators, two full scale experiments were conducted and a third full scale experiment has been planned. Measurements include: brake temperature, tire temperature, engine temperature, vehicle acceleration, engine acoustics, vehicle stability, rear differential temperature and tire height.

The first field test consisted of building and employing on-board and off-board vehicle sensing systems to collect data on all of the aforementioned indicators. The data collection plan was executed at a racetrack to eliminate traffic variables, improve roadside access for the off-board sensors, decrease weight restrictions and maximize the effectiveness and efficiency of the collect. The vehicle that was chosen for use in the first experiment was a 1992 Ford F600 flatbed dump truck with a gross vehicle weight rating (GVWR) of 23,500 lbs and can be seen in Figure 1. This vehicle has a 5.9 liter Cummins 4-stroke diesel engine, manual transmission, split rear-end, disc brakes in the front and drum brakes in the rear. The vehicle was selected because of its varied braking

Figure 1: The 1992 Ford F600 chosen for the first field test.

methods (drum and disc), manual transmission with two speed differential (similar to the transmission found in most tractor-trailers), functioning dump box which allows easy access to the frame for sensor mounting and a high GVWR that is very near the 26,000 lbs limit that requires a commercial driver's license to operate.

The purpose of the on-board sensing system was to measure and record temperatures, acoustic signals, vehicle frame vibration and tire pressure information about the vehicle. Eleven K-Type thermocouples were installed on the truck to measure the temperatures of various components. Six of the thermocouples were installed on the brakes, one bolted to each of the rear brake shoes (4 total) and one bolted to each of the inside front brake pads (2 total). One thermocouple was bolted to the inside of the exhaust pipe. Two thermocouples were affixed to the rear differential using adhesive thermal pads after thoroughly scouring the area with a grinder to expose bare metal. One thermocouple each was installed on the oil pan and the inner cooler using adhesive thermal pads. Two Micro-Epsilon Tim-160 microbolometer thermal imagers were installed to measure the temperature of rotating components; this includes the brake discs, brake drums and tires. One thermal imager was mounted in the front driver's side wheel well directed at the driver's side front brake and tire. The second thermal imager was mounted on the truck frame and was directed at the rear passenger's side brake and tires. In both cases the thermal imagers were installed using adjustable fixtures that allowed nearly 360° of rotation. Two triaxial accelerometers were installed to measure the response of the suspension by comparing the acceleration at the rear axle to the acceleration at the frame. A steel plate and mounting base were welded to both the rear axle and the frame to allow for easy installation and removal of the two triaxial accelerometers. Microphones were installed in the engine compartment directed at the valve train and on the frame directed at the exhaust pipe. The microphones were installed using custom mounting fixtures that allow the position and direction of the microphones to be adjusted easily. Six wireless pressure sensors were installed to measure each tire's pressure. Wires were run from each of the wired components described above to a data acquisition system installed in the cab of the truck. The data acquisition system was used to digitize and store all of the measurement data generated by the on-board sensors. A global positioning system (GPS) receiver was used to synchronize the collection of the on-board data and also generate a trigger signal for a pulsing LED light used to synchronize the off-board measurements with the on-board measurements.

The purpose of the off-board sensing system was to measure and record temperature and acoustic data about the vehicle from a location adjacent to the path of the truck. The system includes the Wildfire Airborne Sensor

Figure 2: The tractor trailer that was chosen for the second full scale test.

Program (WASP)[2] infrared sensor system, two microphones and a high definition video camera. The purpose of the microphones in the off-board system was to determine the difference in signal for an off-board system as compared to an on-board system as well as to investigate the impact of the Doppler Effect as it relates to signal quality. The purpose of the high definition video was to measure the response of the suspension as the truck travels over a standard speed bump and to measure the acceleration and deceleration rates of the vehicle. A data acquisition system was used to digitize and record the signals from the microphones. Both WASP and the high definition camera utilized on-board data storage capabilities.

The test plan that was developed consisted of three different experiments repeated for various truck loads. The first experiment was designed to measure the heat generated by the braking system during a deceleration to a stop from a known velocity over a predetermined distance with the transmission disengaged (clutch in). The second experiment was designed to measure the heat generated by the braking system during a deceleration to a stop from a known velocity over a predetermined distance with the transmission engaged (clutch out). The third experiment was designed to measure the response of the truck's suspension as it travelled over a standard sized speed bump. Each experiment was repeated three times for each of the vehicle loads chosen. Data from both the on-board and off-board sensor systems are collected during the entirety of each test run.

The Wyoming County International Speedway near Rochester, NY was selected as the site of the first data collect. The racetrack is a 1/3 mile asphalt oval track with a mild bank. The track also provided access to several large concrete blocks to load the test vehicle and a nearby calibrated truck scale to weigh the loaded and unloaded test vehicle. Each experiment described in the test plan was completed three times for the following gross vehicle weights; 23,550 lbs, 19,540 lbs, 15,530 lbs and 11,520 lbs.

The second full scale field test took place at the Savannah River Site in Aiken, South Carolina. The vehicle that was chosen for the full scale test was a Western-Star tractor with a 15.2 liter Caterpillar diesel engine pulling a 40 ft three-axle trailer and can be seen in Figure 2. The tractor had a manual transmission, drum brakes and was equipped with a "Jacobs" style exhaust brake. The maximum load for this tractor-trailer combination is approximately 40 tons. The full scale field test employed both on-board and off-board sensor systems. The on-board system consisted of two IR video cameras (Micro-Epsilon Tim-160 microbolometer arrays), two K-type thermocouples, two free-field microphones (PCB Piezotronics) and a Global Positioning System (GPS). The IR video cameras were positioned to monitor the front, passenger-side tractor brake and tire and the rear, driver side tractor tires, brakes and differential. One thermocouple was positioned within the field of view of each of the IR cameras to provide data for calibration. The microphones were positioned on the trailer and directed at the exhaust pipes. The GPS receiver was mounted in the center of the trailer and recorded position data at a 5Hz rate.

The off-board system consisted of two free-field microphones (PCB Piezotronics), two triaxial accelerometers (PCB Piezotronics), a digital SLR camera (Canon T2i used for both video and image capture) and the WASP infrared sensor system. The microphones were mounted near the road and used to gather acoustic pass-by data.

The accelerometers were mounted on railroad tracks to acquire vibration data as the vehicle traversed them. The camera was mounted at various locations that will be detailed in the experiment description.

The testing consisted of four experiments that were repeated multiple times for loads of approximately 40 tons, 20 tons and 0 tons (empty trailer). The first experiment consisted of accelerating the vehicle to a speed of approximately 35 mph. Next, the vehicle would begin braking, during which the WASP sensor would acquire IR imagery. On-board sensors acquired data continuously for all testing. This experiment was repeated using various braking styles; clutch engaged, clutch disengaged, downshifting and "Jacobs" style exhaust braking. The second experiment called for the vehicle to travel over a set of railroad tracks. The vibration response of the railroad tracks was measured by the two triaxial accelerometers and the pass-by acoustic signal was measured by the two off-road microphones. The third experiment called for the vehicle to accelerate aggressively from a stop while the camera captured video of the front suspension response. The camera was placed in the center of the road for this experiment with the vehicle traveling directly at it. The fourth experiment required the vehicle to traverse a speed bump at a driver determined "normal speed" while the off-board mounted camera recorded video.

3. RESULTS/OBSERVATIONS

During the first full scale track test the driver's side front brake (disk) and the passenger side rear brake (drum) of the test vehicle were monitored using a microbolometer array thermal imager as the vehicle decelerated to a complete stop. Three runs with the clutch engaged and three without the clutch engaged were conducted for each of the four vehicle loads for a total of twenty-four runs. An example of the IR data can be seen in Figures 3a and 3b. Temperature values in digital count (DC) were extracted from the IR video frame by frame for both the brakes and the tires. This was done using an intensity based pattern tracking algorithm which tracked the temperature of multiple areas within the scene and recorded the minimum, maximum and average temperature for each region. The regions consisted of a portion of the front disk brake, a portion of the rear drum brake, the front of the rear tires and a portion of the rear differential. Four signals were extracted from each run. The signals are as follows:

- Front Driver Side Disk Brake - Minimum value was used to minimize reflected energy
- Rear Passenger Side Drum Brake - Maximum value was used (Non-reflective but small area)
- Rear Passenger Side Tires - Maximum DC value was used (Non-reflective but small area)
- Rear Differential - Mean DC value was used (Non-reflective and large area)

Each signal was plotted versus time and analyzed. The disk brake temperature signals were decomposed into two values which described the curve: the difference between peak temperature and initial temperature and the difference between final temperature and initial temperature. An example of this can be seen in Figure 4. The drum brake temperature signals were decomposed into a single value which described the curve: final temperature minus initial temperature. An example of this can be seen in Figure 5. The rear passenger side tires' temperature signals were analyzed, but the low signal-to-noise ratio did not allow a characteristic value to be found. The rear differential temperature signals were reduced to a single value which described the curve; final temperature minus initial temperature. An example of this can be seen in Figure 6. The normalized correlation coefficient was calculated for all of the data described above and the kinetic energy of the truck for each run at the time braking began. The kinetic energy of the truck was calculated using the standard kinetic energy relationship[1]

$$KE = \frac{m}{2}V^2 \tag{2}$$

where KE denotes kinetic energy, m the mass of the vehicle and V the velocity of the vehicle. The correlation analysis showed the final temperature minus the initial temperature for the front disk brakes to be the value with the strongest correlation to vehicle kinetic energy with nearly 81% correlation. This result is encouraging,

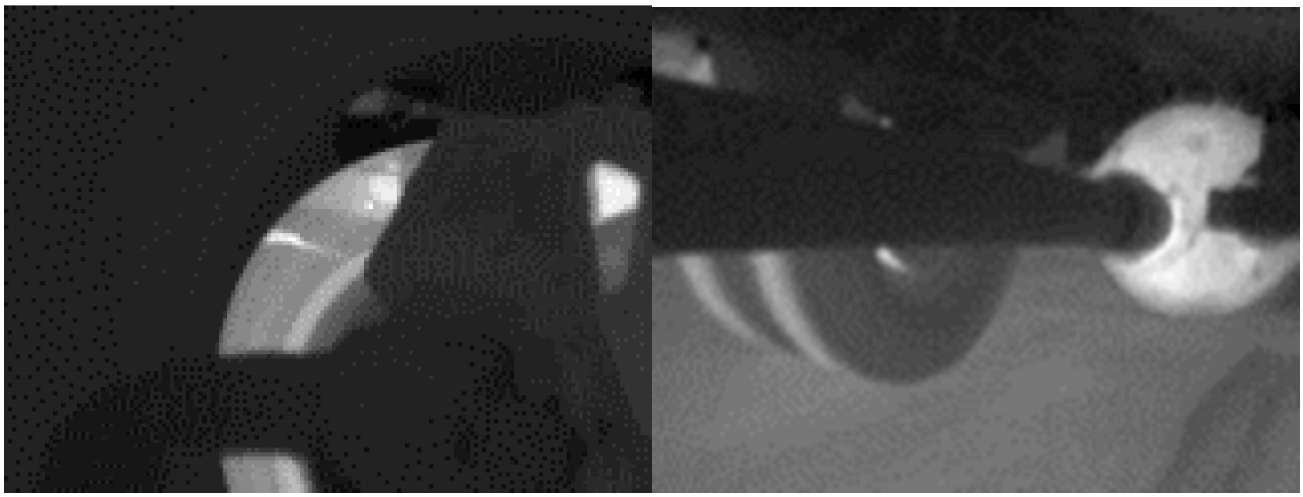

(a) (b)

Figure 3: IR images of (a) the front driver side disk brake (b) from left to right; the rear passenger side tires, the rear passenger side drum brakes, and the rear differential.

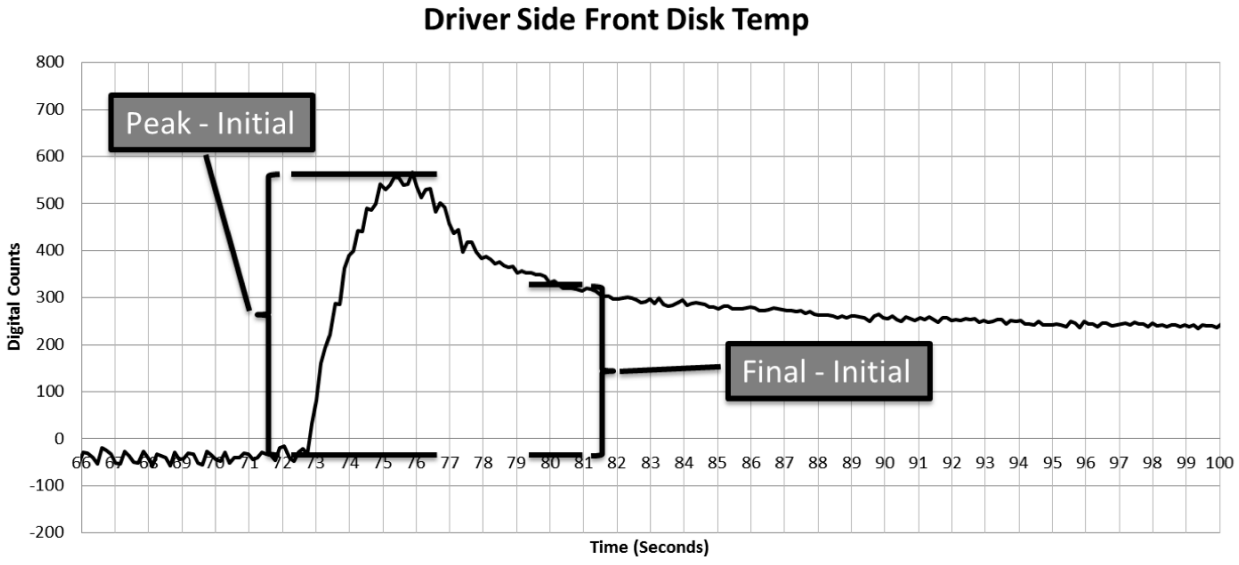

Figure 4: The characteristic values of the driver side front disk temperature signal in digital counts. Note that the final temperature was chosen to be 3 seconds after the vehicle was stopped.

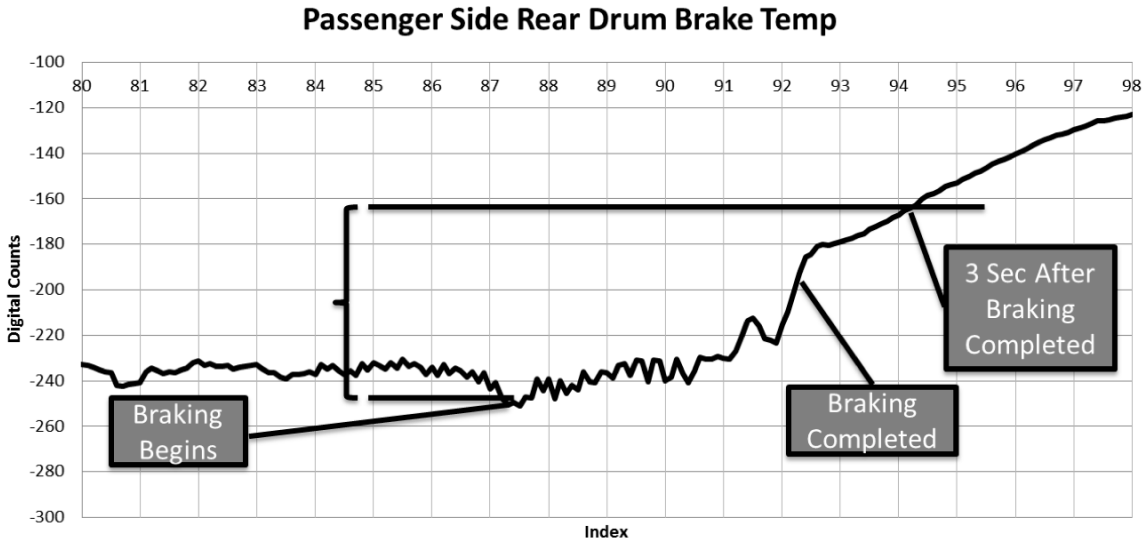

Figure 5: The characteristic values of the passenger side rear drum temperature signal in digital counts. Note that the final temperature was chosen to be 3 seconds after the vehicle was stopped.

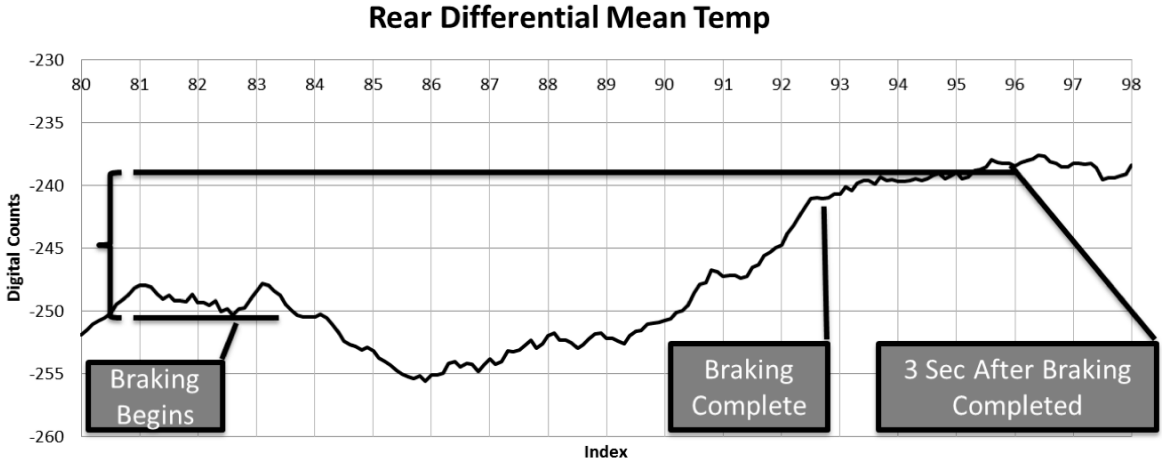

Figure 6: The characteristic values of the rear differential temperature signal in digital counts. Note that the final temperature was chosen to be 3 seconds after the vehicle was stopped.

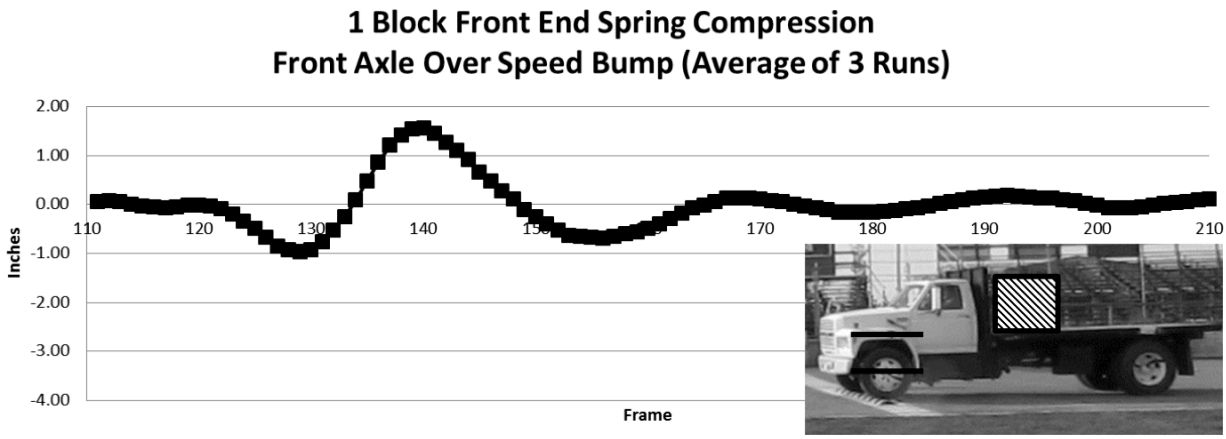

Figure 7: The front suspension compression in inches versus time in seconds for the front axle as the front axle travels over the speed bump.

however, more data is needed to determine if this correlation holds for other vehicles. Similar data from the second full scale track test is currently being processed.

High definition video was obtained during the first full scale track test of the test vehicle as it travelled over a speed bump multiple times. Three runs were conducted for each of the four vehicle loads for a total of twelve runs. The two dimensional coordinates for the center of the driver's side wheels and the vehicle frame fiducials were extracted for each video frame using pattern matching algorithms. Each signal was then rotated to align the x-axis with the axis of vehicle travel and low-pass filtered. The distance between the frame and the wheel was calculated for both the front and rear axle. This resulted in two signals for each run, a signal for the front suspension and for the rear suspension, each plotting the suspension compression versus time. Each signal was then split into two non-overlapping signals so as to differentiate between when the front axle and when the rear axle travelled over the speed bump. An example of this can be seen in Figure 7. The frequency power spectrum of the spring compression data was then calculated. An example of this can be seen in Figure 8. The centroid and area under the curve of the frequency power spectrum was then calculated. An example of this can be seen in Figures 9 and 10. The resulting data for each run can be seen in Table 1. The normalized correlation coefficient was calculated for the matrix and can be seen in Table 2. The correlation analysis showed the total power spectral density of the front suspension as the rear wheels travel over the speed bump to be the indicator with the strongest correlation to vehicle load, nearly 0.95. There is also a 0.76 correlation between vehicle weight and speed. This correlation is an artifact of variability in driver behavior. Multivariate correlation between vehicle weight, speed and total power spectral density (PSD) of the front suspension as the rear wheels passed over the bump showed that the speed effect on the weight - PSD correlation was small. Removal of the spurious speed effect reduced the correlation coefficient from 0.95 to a still highly significant 0.89. Similar data from the second full scale track test is currently being processed.

During the full scale track testing, conducted at the Savannah River Site, a tractor-trailer was loaded with loads of approximately 40 tons, 20 tons and 0 tons (empty trailer). High resolution images were obtained for the outermost passenger side tire for each axle and each load using a Canon T2i 18 megapixel camera. The images were post processed to automatically locate and isolate the wheel using a variation of a method developed by Hutter and Brewer.[3] First the image was converted to grayscale (Figure 11a) and high-pass filtered (Figure 11b). The image was then thresholded (Figure 11c) and all but the largest connected regions were discarded (Figure 11d). A morphological closing was applied to each of the remaining regions (Figure 11e) and a flood fill function was then applied (Figure 11f). The relationship below was then used to quantify how elliptical each region was.

$$E = \frac{1 - N\pi\sqrt{|\Sigma_{xy}|}}{4\pi\sqrt{|\Sigma_{xy}|}} \tag{3}$$

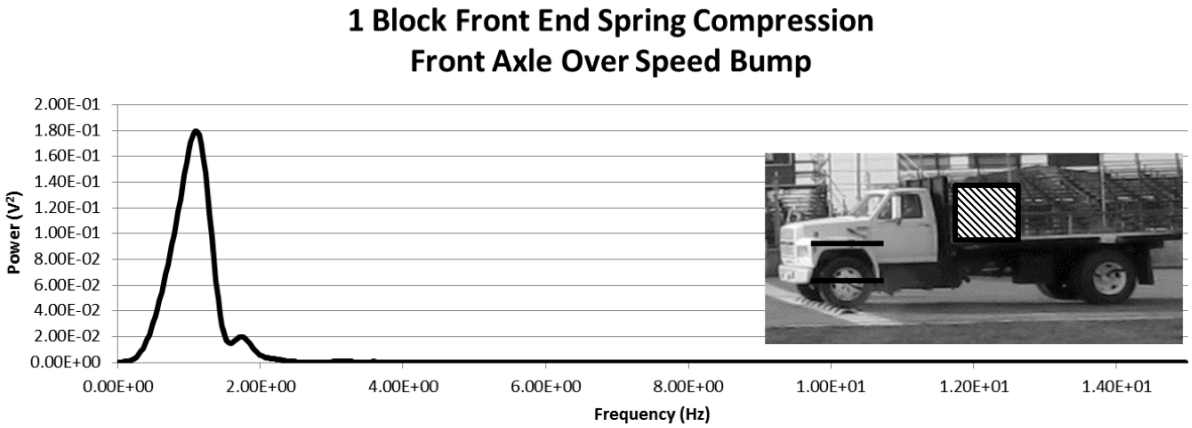

Figure 8: The frequency power spectrum of the spring compression data for the front axle as the front axle travels over the speed bump.

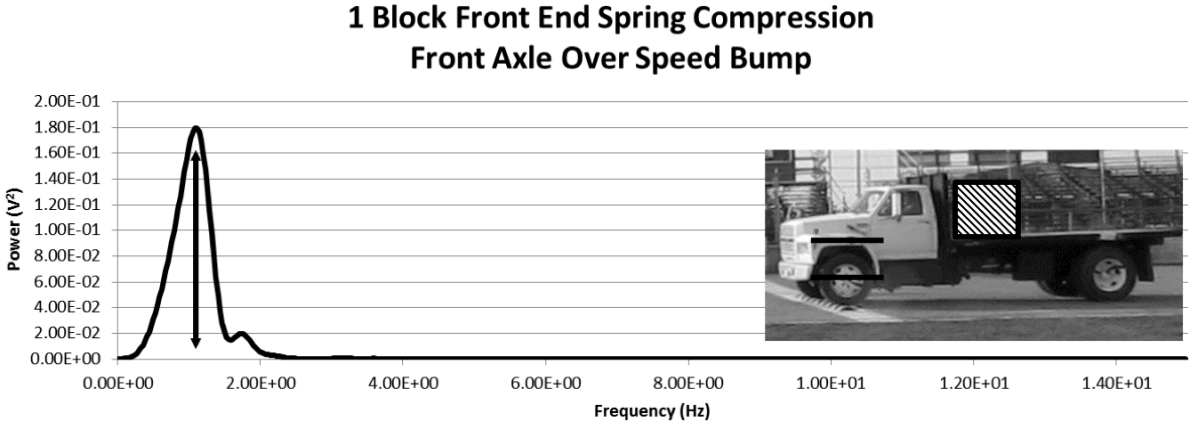

Figure 9: The centroid of the frequency power spectrum of the spring compression data for the front axle as the front axle travels over the speed bump.

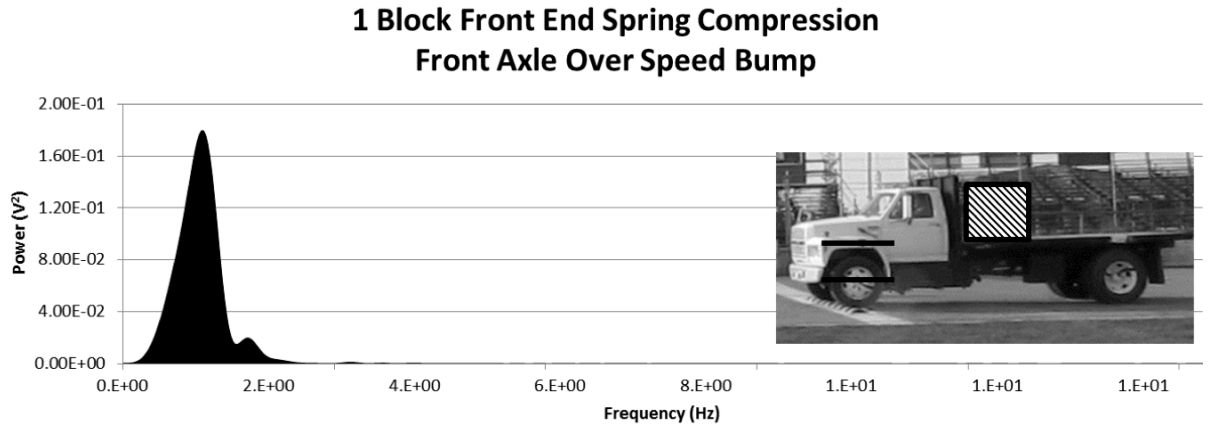

Figure 10: The area under the curve of the frequency power spectrum of the spring compression data for the front axle as the front axle travels over the speed bump.

Table 1: The analysis data from each of the suspension test runs.

Load (T)		Centroids (Hz)				Total PSD				Speed ($\frac{m}{s}$)
		Front End Front Bump	Front End Rear Bump	Front End Rear Bump	Rear End Rear Bump	Front End Front Bump	Rear End Front Bump	Front End Rear Bump	Rear End Rear Bump	
1	11500	1.170	0.453	0.906	1.140	0.071	0.021	0.011	0.040	2.466
2	11500	1.111	0.409	1.199	1.243	0.074	0.028	0.006	0.038	2.619
3	11500	1.096	0.468	0.497	1.374	0.086	0.021	0.010	0.040	2.507
1	15500	0.994	0.526	0.965	1.550	0.106	0.016	0.047	0.041	2.684
2	15500	1.053	0.848	0.936	1.637	0.118	0.011	0.036	0.037	2.448
3	15500	1.053	0.936	0.965	1.491	0.106	0.016	0.042	0.053	2.761
1	19500	0.965	0.673	1.053	1.374	0.081	0.009	0.057	0.020	2.777
2	19500	0.936	0.614	1.023	1.170	0.105	0.014	0.054	0.018	2.519
3	19500	1.023	0.526	1.023	1.316	0.074	0.015	0.057	0.021	2.670
1	23500	0.994	0.702	1.023	1.111	0.098	0.007	0.062	0.021	2.815
2	23500	1.053	0.526	0.906	1.404	0.098	0.013	0.076	0.024	2.943
3	23500	0.994	0.556	1.053	1.053	0.101	0.015	0.063	0.021	2.957

Table 2: The results of the suspension test data correlation analysis.

Parameter	Correlation Coefficient (Weight of Truck)	Probability (Random)
Weight of Truck	1	0
Centroid of Spectrum for Front Suspension as Front Axle Travels Over the Speed Bumps	-0.694	0.012
Centroid of Spectrum for Rear Suspension as Front Axle Travels Over the Speed Bumps	0.209	0.514
Centroid of Spectrum for Front Suspension as Rear Axle Travels Over the Speed Bumps	0.320	0.310
Centroid of Spectrum for Rear Suspension as Rear Axle Travels Over the Speed Bumps	-0.294	0.353
Total PSD of Front Suspension as Front Axle Travels Over the Speed Bumps	0.325	0.302
Total PSD of Rear Suspension as Front Axle Travels Over the Speed Bumps	-0.756	0.004
Total PSD of Front Suspension as Rear Axle Travels Over the Speed Bumps	0.947	0.000
Total PSD of Rear Suspension as Rear Axle Travels Over the Speed Bumps	-0.767	0.004
Speed	0.762	0.004

where E denotes how elliptical the binary region is, N the number of pixels in the region and Σ_{xy} the covariance matrix of the pixel locations in the region of interest. If the region is not elliptical enough to meet user defined criteria the process is repeated with an incrementally larger thresholding value. Finally, the most elliptical region is selected as the wheel (Figure 11g).

The next step in the process was to transform the image so everything in the two-dimensional plane of the wheel/tire interface was perpendicular to the optical axis of the camera. This would enable us to measure the tire deflection in physical units of length. However, determining the proper matrix needed to accurately perform this transformation proved to be more challenging than initially anticipated. Rather than pursue this path it was deemed more efficient to proceed with a camera array (three Canon T2i 18 megapixel cameras taking concurrent images) instead of a single camera for future collects. A camera array would make the deflection measurement much less complicated and should improve the accuracy. Assuming the deflection measurements can be made using the camera array, the weight of the vehicle can be estimated using the equation for stiffness (K) below[4] and some basic assumptions about the tire composition, construction and inflation pressure (P)

$$K = 0.00028P\sqrt{\left(-0.004R_A + 1.03\right) S_N \left(\frac{S_N R_A}{50} + D_R\right)} + 3.45 \tag{4}$$

The aspect ratio (R_A) is equal to 100 times tire height (unloaded) divided by the section width of the tire (S_N) and can be calculated from basic tire measurements or read off the sidewall of the tire. The rim diameter D_R can also be measured or read off the sidewall of the tire. With tire stiffness and tire deflection the vehicle weight can be calculated. Independent field testing is planned to quantify the precision and accuracy of this method.

Vibration and high resolution video data was collected during the full scale test at the Savannah River Site as the tractor-trailer traveled over a set of railroad tracks multiple times for each load. The vibration data was collected using two triaxial accelerometers (one mounted to each rail) and the video data was collected using a Canon T2i camera. Before the accelerometer data was processed it was important to develop a method to determine the distance between the tire and the accelerometer in each image so the accelerometer data could be properly scaled. First the video was converted into a set of individual frames and twelve frames were extracted

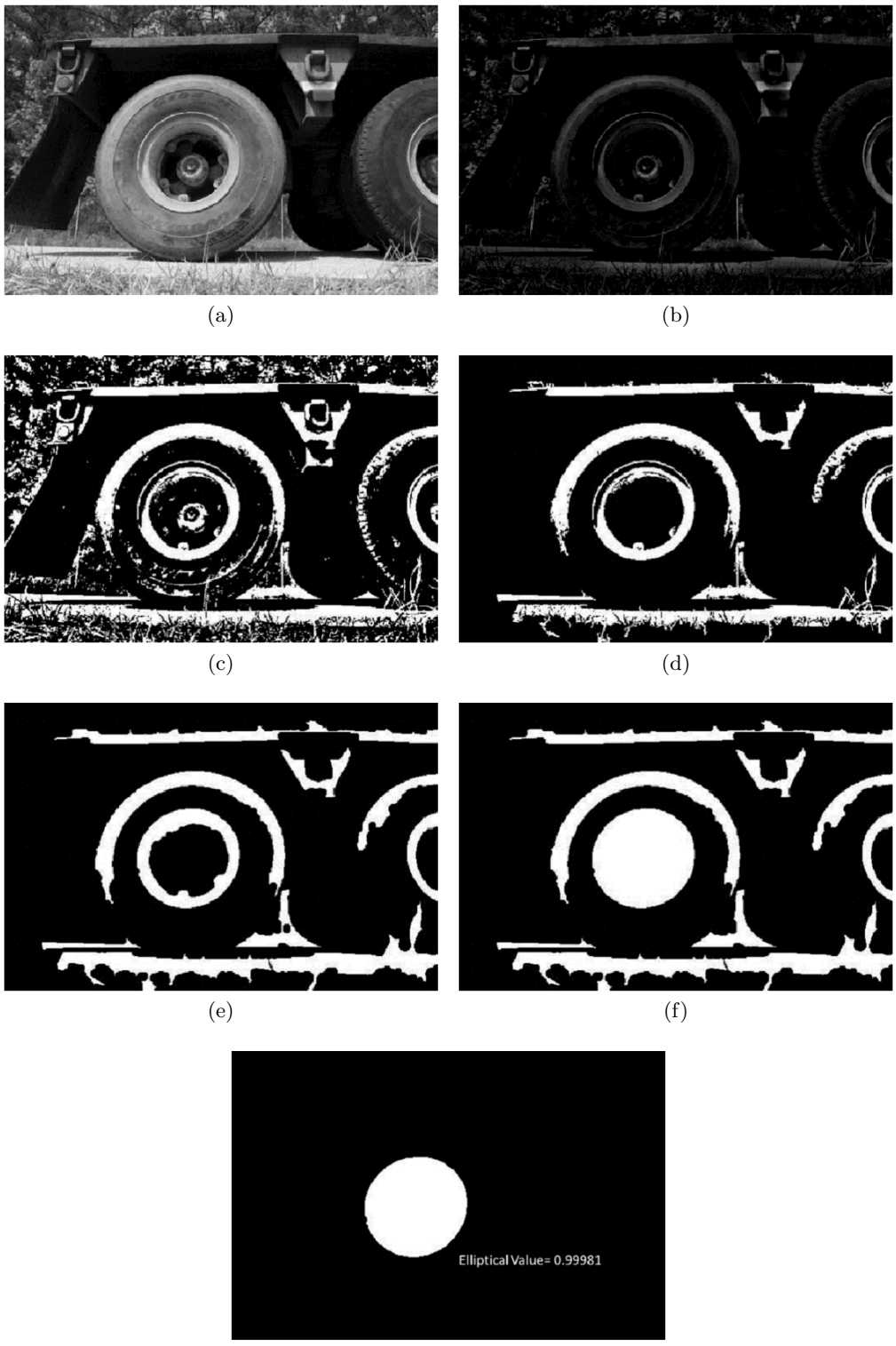

(a) (b) (c) (d) (e) (f) (g)

Figure 11: The original color image was converted to grayscale (a), high pass filtered (b), thresholded (c), then the small regions were removed (d), morphologically closed (e), flood filled (f) and finally the most elliptical region was selected (g)

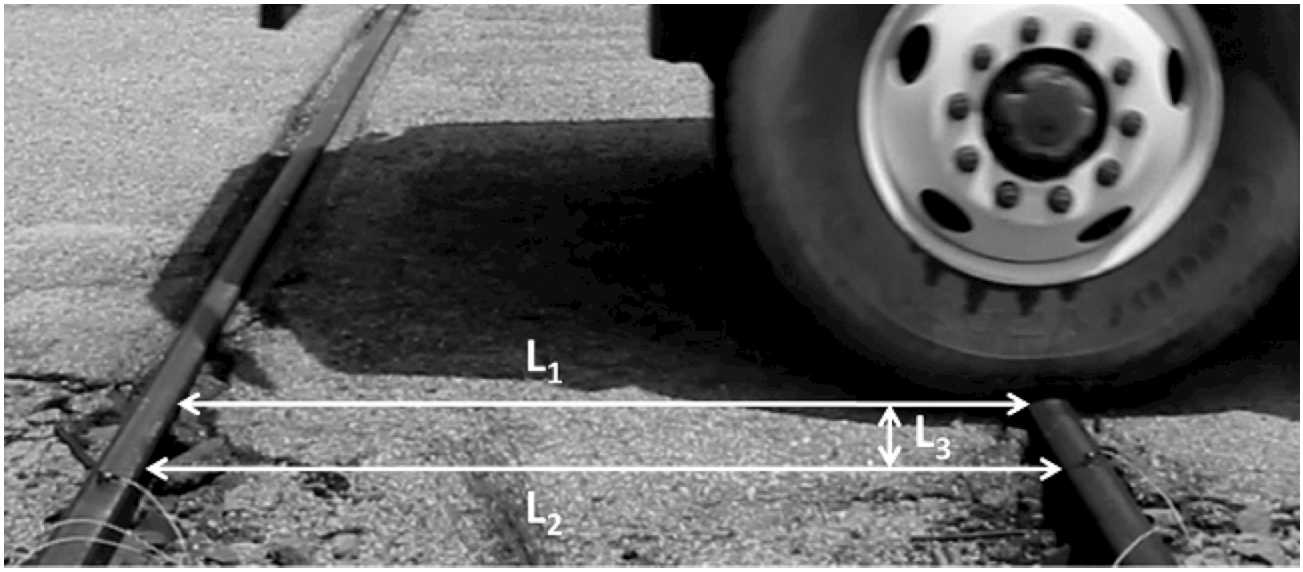

Figure 12: The physical distance from the vehicle's tire to the accelerometer, d, was calculated using the distances L_1 L_2 and L_3 in pixels and knowledge of the physical distance between standard railroad tracks.

from each run. Each of the twelve frames were associated with one of the six vehicle wheels centered on one of the railroad tracks. Values for L_1, L_2 and L_3 from Figure 12 were measured from the image in pixels by the user and the distance, in meters, between the tire and accelerometer was calculated using the relationship below.

$$d = \frac{L_0 f}{p}\sqrt{\frac{1}{L_1^2} + \frac{1}{L_2^2} - \frac{2cos\left(2tan^{-1}\left(\frac{pL_3}{2f}\right)\right)}{L_1 L_2}} \tag{5}$$

where d denotes the distance between the tire and the sensor in meters, L_0 the distance between tracks for a standard railroad in meters, f the camera focal length in meters, p the camera's pixel pitch in meters and L_1, L_2 and L_3 measured in pixels and labeled in Figure 12. The physical values focal length (f), pixel pitch (p) and the distance between rails (L_0) must be known.

The next step was to process the accelerometer data for each axle. The data was low-pass filtered (2 Hz) and high-pass filtered (4000 Hz) per the sensor's technical specifications. Then, the tri-axial data was combined into a magnitude using the root mean square (RMS) method the signal associated with each axle was extracted (this was done to isolate the energy by axle). Next, the translational speed of each of the axles was calculated as they traversed the railroad tracks. This was done using the time between impacts and the known distance between the tracks. Finally, the area under the curve (AUC) was calculated for each signal and the peak was located for the Fast Fourier Transform (FFT) of each signal.

The resulting processed data from each of the railroad track test runs can be seen in Table 3. The normalized correlation coefficient was calculated for the matrix and the results can be seen in Table 4. The results show a strong correlation between many of the calculated values from the railroad test runs. Unfortunately the data also shows a strong negative correlation between the sensor to tire distance and the kinetic energy of the vehicle. This tells us that the driver consistently drove closer to the sensors when the tractor trailer was fully loaded than he did when the truck was unloaded. This may be driving some of the correlation we observed and more data will be needed to quantify the significance. The data also shows strong correlation between vehicle speed and nearly all of the other indicators. Further investigation will need to be done to understand the role vehicle speed plays in the transfer of energy from vehicle to railroad track.

Table 3: Data calculated from each of the railroad track test runs

Load (T)	Run	Avg Dist (m)	Speed ($\frac{m}{s}$)	Energy (J)	Peak (g)	Norm Peak ($\frac{g}{r}$)	Norm Peak ($\frac{g}{r2}$)	AUC (gs)	Norm AUC ($\frac{gs}{r}$)	Norm AUC ($\frac{gs}{r^2}$)	FFT Peak	Norm FFT $\frac{Peak}{r}$	Norm FFT $\frac{Peak}{r^2}$
40	2	0.36	2.14	207470	2.23	6.13	16.86	0.06	0.16	0.44	0.05	0.13	0.37
40	3	0.37	1.73	135146	1.64	4.45	12.06	0.06	0.16	0.42	0.03	0.09	0.26
40	4	0.34	1.85	154457	1.78	5.27	15.60	0.06	0.18	0.52	0.04	0.12	0.35
40	5	0.36	1.99	178862	1.69	4.75	13.36	0.06	0.17	0.48	0.04	0.12	0.35
20	2	0.40	1.77	85231	1.70	4.23	10.52	0.06	0.14	0.35	0.04	0.09	0.22
20	3	0.38	2.35	149947	2.35	6.15	16.12	0.06	0.17	0.44	0.06	0.16	0.41
20	4	0.42	2.10	120282	2.00	4.76	11.33	0.06	0.13	0.32	0.05	0.11	0.26
0	1	0.72	1.73	27174	1.09	1.52	2.12	0.05	0.07	0.09	0.03	0.04	0.06
0	2	0.69	1.59	23045	1.33	1.94	2.83	0.05	0.08	0.11	0.03	0.04	0.06
0	3	0.71	1.69	25827	1.19	1.68	2.38	0.05	0.07	0.10	0.03	0.04	0.06
0	4	0.74	1.56	21966	0.82	1.11	1.49	0.04	0.05	0.07	0.02	0.03	0.04
0	5	0.71	1.65	24791	0.94	1.33	1.86	0.04	0.06	0.09	0.03	0.04	0.05

Table 4: The results of the railroad track test data correlation analysis.

	Load (T)	Run	Avg Dist (m)	Speed ($\frac{m}{s}$)	Energy (J)	Peak (g)	Norm Peak ($\frac{g}{r}$)	Norm Peak ($\frac{g}{r2}$)	AUC (gs)	Norm AUC ($\frac{gs}{r}$)	Norm AUC ($\frac{gs}{r^2}$)	FFT Peak	Norm FFT $\frac{Peak}{r}$
Load (T)	1.00												
Run	0.17	1.00											
Avg Dist (m)	-0.93	-0.12	1.00										
Speed ($\frac{m}{s}$)	0.54	0.04	-0.70	1.00									
Energy (J)	0.94	0.15	-0.93	0.78	1.00								
Peak (g)	0.72	-0.10	-0.87	0.90	0.86	1.00							
Norm Peak ($\frac{g}{r}$)	0.86	0.03	-0.96	0.85	0.95	0.96	1.00						
Norm Peak ($\frac{g}{r^2}$)	0.91	0.08	-0.97	0.80	0.97	0.93	0.99	1.00					
AUC (gs)	0.79	-0.03	-0.91	0.76	0.85	0.91	0.92	0.91	1.00				
Norm AUC ($\frac{gs}{r}$)	0.93	0.12	-0.99	0.72	0.94	0.87	0.96	0.98	0.94	1.00			
Norm AUC ($\frac{gs}{r^2}$)	0.95	0.16	-0.98	0.68	0.95	0.84	0.95	0.97	0.91	1.00	1.00		
FFT Peak	0.63	0.05	-0.79	0.99	0.83	0.94	0.91	0.87	0.84	0.81	0.78	1.00	
Norm FFT $\frac{Peak}{r}$	0.82	0.11	-0.92	0.90	0.94	0.95	0.98	0.97	0.91	0.94	0.93	0.96	1.00
Norm FFT $\frac{Peak}{r^2}$	0.88	0.14	-0.95	0.85	0.96	0.92	0.98	0.99	0.91	0.97	0.96	0.91	0.99

4. CONCLUSIONS

The experiments designed and executed during this study have provided the authors with a large multivariate data set. To date, we have identified several promising indicators that show strong correlation to vehicle weight; tire deflection, suspension response and railroad response. We are expecting to modify our list of indicators to the most promising few, and investigate them further by executing a third, more narrowly focused, field test.

The last stage of this research will be to statistically analyze the results of the third field test and determine the best way to combine the different indicators into an accurate method of determining vehicle weight.

ACKNOWLEDGMENTS

The authors would like to thank the United States Department of Energy for their support of this effort under contract number DE-AC09-08SR22470/AC799980.

REFERENCES

1. D. Halliday, R. Resnick, and J. Walker, "Fundamentals of physics," 2005.
2. D. McKeown, J. Cocburn, J. Faulring, K. Kremens, D. Morse, H. Rhody, and M. Richardson, "Wildfire airborne sensor program (WASP): A new wildland fire detection and mapping system," in *Proceedings of the Tenth Forest Service Remote Sensing Applications Conference*, pp. 5–9, 2004.
3. M. Hutter and N. Brewer, "Matching 2-d ellipses to 3-d circles with application to vehicle pose identification," in *Image and Vision Computing New Zealand, 2009. IVCNZ'09. 24th International Conference*, pp. 153–158, IEEE, 2009.
4. T. Rhyne, "Development of a vertical stiffness relationship for belted radial tires," 2005.